Supporting Information

Stable cationic nanobelts synthesized by chemical oxidation of methylene-bridged [6]cycloparaphenylene

Nobushige Kai,[a,+] Hideya Kono,[a,+] Timo Stünkel,[a] Daiki Imoto,[a] Riccardo Zanasi,[b,*] Guglielmo Monaco,[b] Francesco F. Summa,[b] Lawrence T. Scott,[c] Akiko Yagi,[a,d,*] and Kenichiro Itami[d,e,*]

[a] Department of Chemistry, Graduate School of Science, Nagoya University, Chikusa, Nagoya 464-8602, Japan

[b] Dipartimento di Chimica e Biologia "A. Zambelli", Università degli Studi di Salerno, Fisciano 84084, SA, Italy.

[c] Department of Chemistry, University of Nevada, Reno, Nevada 89557-0216, USA.

[d] Institute of Transformative Bio-Molecules (WPI-ITbM), Nagoya University, Nagoya 464-8602, Japan.

[e] Molecule Creation Laboratory, RIKEN Cluster for Pioneering Research, RIKEN, Wako, Saitama 351-0198, Japan

[+] These authors contributed equally.

*E-mail: rzanasi@unisa.it (R.Z.), yagi.akiko@itbm.nagoya-u.ac.jp (A.Y.), kenichiro.itami@riken.jp (K.I.)

Table of Contents

Supplementary Methods

1. Materials and methods

Materials: Unless otherwise noted, all reactants or reagents including dry solvents were obtained from commercial suppliers and used as received. Unless otherwise noted, all reactions were performed with dry solvents under an atmosphere of nitrogen in dried glassware using standard vacuum-line techniques. Unless otherwise noted, all work-up and purification procedures were carried out with reagent-grade solvents under air.

MS, NMR and ESR: The high-resolution mass spectra (HRMS) were obtained from Bruker Daltonics compact (ESI). Nuclear magnetic resonance (NMR) spectra were recorded on a JEOL JNM-ECA-600 (^{1}H 600 MHz, ^{13}C 150 MHz) spectrometer and a JEOL ECA 600 II spectrometer equipped with a UltraCOOL probe. Chemical shifts for ^{1}H NMR are expressed in parts per million (ppm) relative to residual $CHDCl_2$ (δ 5.32 ppm). ^{13}C NMR spectra were recorded using a proton-decoupled pulse sequence. Chemical shifts for ^{13}C NMR are expressed in ppm relative to CD_2Cl_2 (δ 54.0 ppm) or $C_2D_2Cl_4$ (δ 73.78 ppm). Data are reported as follows: chemical shift, multiplicity (s = singlet, d = doublet), coupling constant (Hz), and integration. Electron paramagnetic resonance (EPR) spectra were recorded on JEOL ESR JES-X320 instruments using quartz Schlenk tube filled with argon.

X-ray crystallography: Details of the crystal data and a summary of the intensity data collection parameters for **2** are listed in Table S1. A suitable crystal was mounted with mineral oil on a MiTeGen MicroMounts and transferred to the goniometer of the kappa goniometer of a RIGAKU XtaLAB Synergy-S system with 1.2 kW MicroMax-007HF microfocus rotating anode (Graphite-monochromated Mo Kα radiation (λ = 0.71073 Å)) and PILATUS200K hybrid photon-counting detector. Cell parameters were determined and refined, and raw frame data were integrated using CrysAlis^{Pro} (Agilent Technologies, 2010). The structures were solved by direct methods with SHELXT[S1] and refined by full-matrix least-squares techniques against F^2 (SHELXL-2018/3)[S2] by using Olex2 software package.[S3] The intensities were corrected for Lorentz and polarization effects. The non-hydrogen atoms were refined anisotropically. Hydrogen atoms were placed using AFIX instructions. CCDC 2359239 contains the supplementary crystallographic data for **2**. These data can be obtained free of charge from The Cambridge Crystallographic Data Centre via www.ccdc.cam.ac.uk/data_request/cif.

Photophysical measurements: UV–vis absorption spectra were recorded on a Shimadzu UV-3600 spectrometer with a resolution of 0.5 nm. Dilute solutions in spectral grade dichloromethane in a 1 cm square quartz cell were used for measurements. Emission spectra were recorded on a were recorded with a JASCO FP-6600 fluorescence spectrometer with a resolution of 0.4 nm. Absolute quantum yields (Φ) were determined with a Quantaurus-QY Plus C-13534-

02 (Hamamatsu Photonics) equipped with NIR PL measurement unit C13684-01 calibrated with an integrating sphere system.

Computational study: The Gaussian 16 program[S4] running on a NEC LX 110Rh system was used for optimization (B3LYP/6-31G(d).[S5,S6] Structures were optimized without any symmetry assumptions. Zero-point energy, enthalpy, and Gibbs free energy at 298.15 K and 1 atm were estimated from the gas-phase studies. Harmonic vibration frequency calculation at the same level was performed to verify all stationary points as local minima (with no imaginary frequency). Also GIAO-NMR and CSGT-NMR were calculated using the B3LYP/6-311+G(2d,p) with SMD (CH_2Cl_2) model.

2. Synthesis of [6]MCPP cations

2.1 Synthesis of 1 and 1′

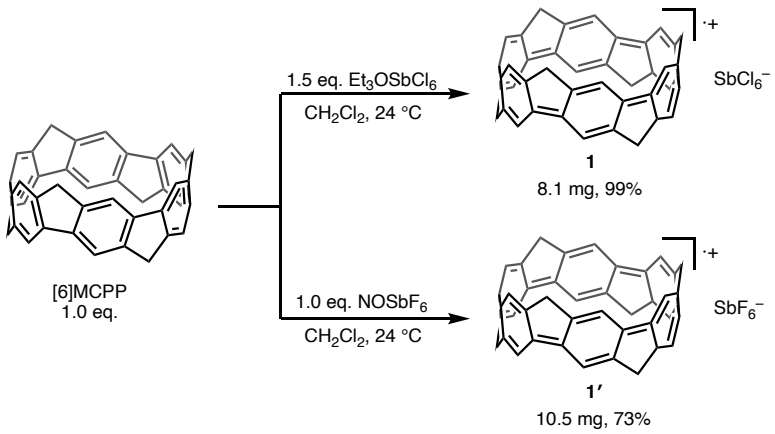

To an oven dried 50-mL vial containing a magnetic stirring bar was added [6]MCPP (9.6 μmol, 5.1 mg, 1.0 eq.). The vial was degassed and placed inside the glove box and added dichloromethane 2.0 mL, which was degassed by freeze-pump-thaw cycles. Et_3OSbCl_6 (14 μmol, 6.2 mg, 1.5 eq.) in dichloromethane 2.0 mL were added to the vial and stirred for 30 minutes at r.t. Hexane 4.0 mL was added to the reaction mixtures. The resulting precipitate was collected by filtration and washed with hexane/CH_2Cl_2 = 1:1 to give the oxidized product **1** (8.1 mg, 99%) as a black solid. Identification of **1** was concluded from its absorption spectrum and ESR spectrum (see Figure S5 and Figure S14, respectively).

To an oven dried 50-mL vial containing a magnetic stirring bar was added [6]MCPP (19 μmol, 10.1 mg, 1.0 eq.). The vial was degassed and placed inside the glove box and added dichloromethane 4.0 mL, which was degassed by freeze-pump-thaw cycles. $NOSbF_6$ (19 μmol, 5.0 mg, 1.0 eq.) in dichloromethane 4.0 mL were added to the vial and stirred for 2 hours at 24 ºC. Hexane 8.0 mL was added to the reaction mixtures. The resulting precipitate was collected by filtration and washed with hexane/CH_2Cl_2 = 1:1 to give the oxidized product **1′** (10.5 mg, 73%) as a black solid. Identification of **1′** was concluded from its ESR spectrum (see Figure S14).

2.2 Synthesis of 2

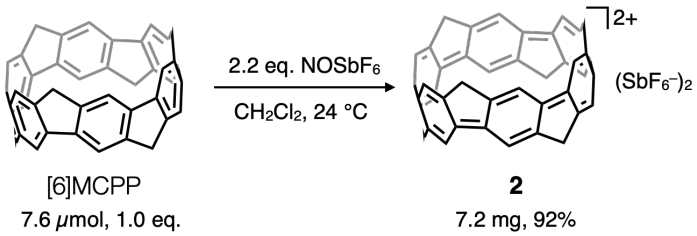

To a dried 10-mL two-neck round-bottom flask containing a magnetic stirring bar was added [6]MCPP (7.6 μmol, 4.0 mg, 1.0 eq.). The vial was degassed and placed inside the glove box. $NOSbF_6$ (23 μmol, 6.0 mg, 3.0 eq.) and dichloromethane 3.0 mL, which was degassed by freeze-pump-thaw cycles, were added to the vial and stirred for 2 hours at 24 °C. The vial was brought out to air and dark green colored reaction mixtures were filtered off by Celite® and then concentrated *in vacuo* to ca. 10 mL, and hexane (ca. 200 mL) was added. The resulting precipitate was collected by filtration to give the product **2** (7.2 mg, 92%) as a dark blue solid.

^{1}H NMR (600 MHz, CD_2Cl_2) δ (ppm) 4.18 (s, 12H), 3.61 (d, J = 18.0 Hz, 6H), –0.34 (d, J = 18.6 Hz, 6H).
^{13}C NMR (150 MHz, $C_2D_2Cl_4$) δ (ppm) 164.91, 161.15, 123.69, 36.25.
HRMS (ESI, positive) *m/z* calcd for $C_{42}H_{24}$ $[M]^{2+}$: 264.0934, found: 264.0923.

2.3 Synthesis of 3

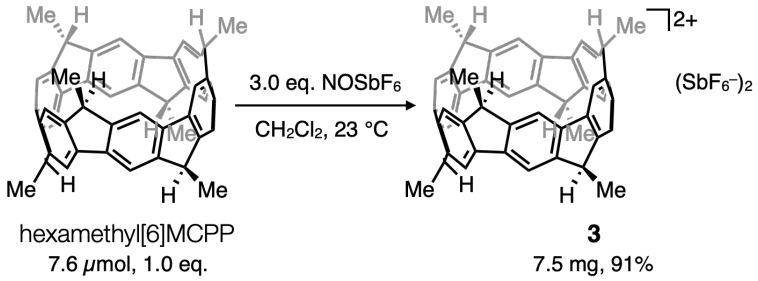

To a dried 10-mL two-neck round-bottom flask containing a magnetic stirring bar was added hexamethyl[6]MCPP (7.6 μmol, 4.6 mg, 1.0 eq., synthesized by following reported procedure[S7]). The vial was degassed and placed inside the glove box. $NOSbF_6$ (23 μmol, 6.0 mg, 3.0 eq.) and dichloromethane 3.0 mL, which was degassed by freeze-pump-thaw cycles, were added to the vial and stirred for 2 hours at 23 °C. The vial was brought out to air and dark green colored reaction mixtures were filtered off by Celite® and then concentrated *in vacuo* to ca. 10 mL, and hexane (ca. 200 mL) was added. The resulting precipitate was collected by filtration to give the oxidized products **3** (7.5 mg, 91%) as a dark blue solid.

^{1}H NMR (600 MHz, CD_2Cl_2) δ (ppm) 4.17 (s, 12H), 1.95 (d, J = 7.2 Hz, 18H), –0.12 (q, J = 13.8 Hz, 7.2 Hz, 6H).

^{13}C NMR spectrum was not obtained. Even in a saturated solution, the concentration was insufficient.

HRMS (ESI, positive) *m/z* calcd for $C_{48}H_{36}$ $[M]^{2+}$: 306.1403, found: 306.1414.

2.4 The comproportionating reaction by mixing 2 and neutral [6]MCPP

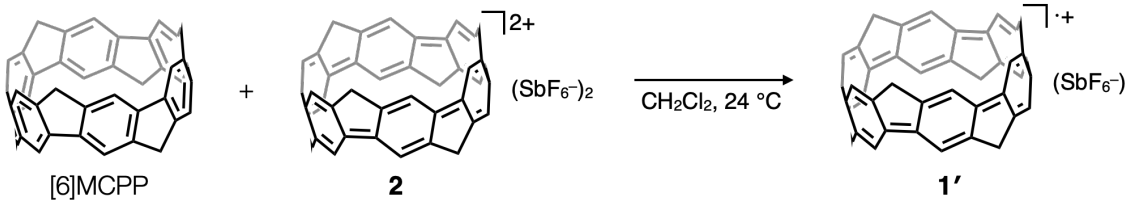

[6]MCPP | **2** | **1′**

2.1 μmol, 1.0 eq. | 2.1 μmol, 1.0 eq. | 3.1 mg, 97%

To an oven dried 30-mL vial containing a magnetic stirring bar was added [6]MCPP (2.1 μmol, 1.1 mg, 1.0 equiv). The vial was degassed and placed inside the glove box and added dichloromethane 1.0 mL, which was degassed by freeze-pump-thaw cycles. **2** (2.1 μmol, 2.1 mg, 1.0 equiv) in dichloromethane 1.0 mL were added to the vial and stirred for 30 minutes at r.t. Hexane 4.0 mL was added to the reaction mixtures. The resulting precipitate was collected by filtration and washed with hexane/CH_2Cl_2 = 1:1 to give the oxidized product **1′** (3.1 mg, 97%) as a black solid. Identification of **1′** was concluded from its absorption spectrum.

Supplementally Figures and Tables

1. Half-life time of 1, 2, 3 (regarding Scheme 1 in the main text)

The stability of **1, 2** and **3** in solution phase under air was respectively investigated by using the dichloromethane solution (5.68×10^{-5} M at 293 K). The UV–vis–NIR absorption spectra were measured every one hour (Figure S1a, S2a, S3a). The half-life time was elucidated from the scheme below based on the decrease of the absorption maximum peak (Figure S1b, S2b, S3b).

$$N = N_0 \left(\frac{1}{2}\right)^{\frac{t}{T}}$$

$$\log_{10} \frac{N}{N_0} = -\frac{\log 2}{T} \times t$$

N_0: The maximum absorbance at starting time; N_t: The maximum absorbance at time t.

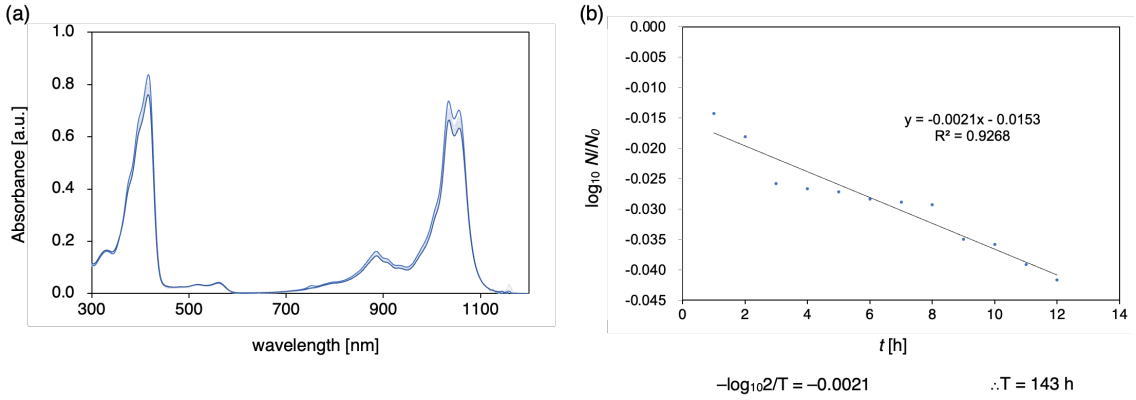

Figure S1. (a) Time-dependence of the absorption spectra of **1**. (b) Plots for half-life of **1** in CH_2Cl_2 solution (monitored at 415 nm).

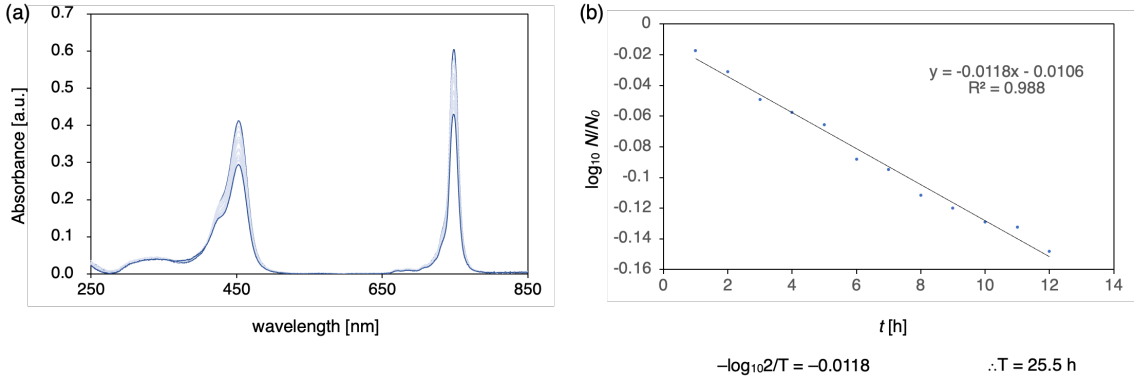

Figure S2. (a) Time-dependence of the absorption spectra of **2**. (b) Plots for half-life of **2** in CH_2Cl_2 solution (monitored at 745 nm).

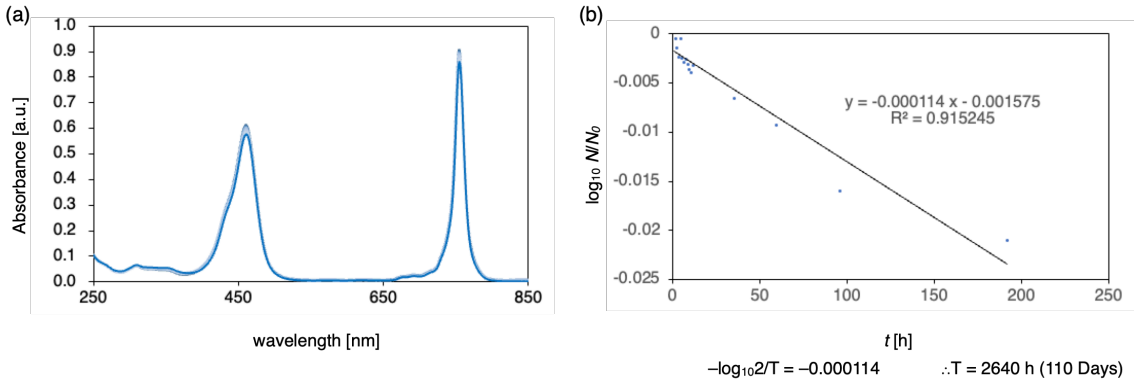

Figure S3. (a) Time-dependence of the absorption spectra of **3**. (b) Plots for half-life of **3** in CH_2Cl_2 solution (monitored at 755 nm).

2. X-ray crystallography (regarding Figure 2 in the main text)

Table S1. Crystallographic data and structure refinement details of **2**.

	2
CCDC No.	2359239
formula	$C_{47}H_{34}Cl_{10}F_{12}Sb_2$
fw	1424.74
T (K)	123(2)
λ (Å)	0.71073
cryst syst	triclinic
space group	P-1
a (Å)	11.0560(3)
b (Å)	12.0361(2)
c (Å)	12.1017(3)
α (deg)	105.769(2)
β (deg)	104.054(2)
γ (deg)	116.448(2)
V (Å^3)	1257.78(6)
Z	1
D_{calc} (g·cm^{-3})	1.881
μ (mm^{-1})	1.685
F(000)	696.0
cryst size (mm^3)	0.18 × 0.08 × 0.01
2θ range (deg)	3.858–59.842
reflns collected	19722
indep reflns/R_{int}	5972 / 0.0354
params	334
GOF on F^2	1.040
R_1, wR_2 [$I>2\sigma(I)$]	0.0259, 0.0629
R_1, wR_2 (all data)	0.0290, 0.0639

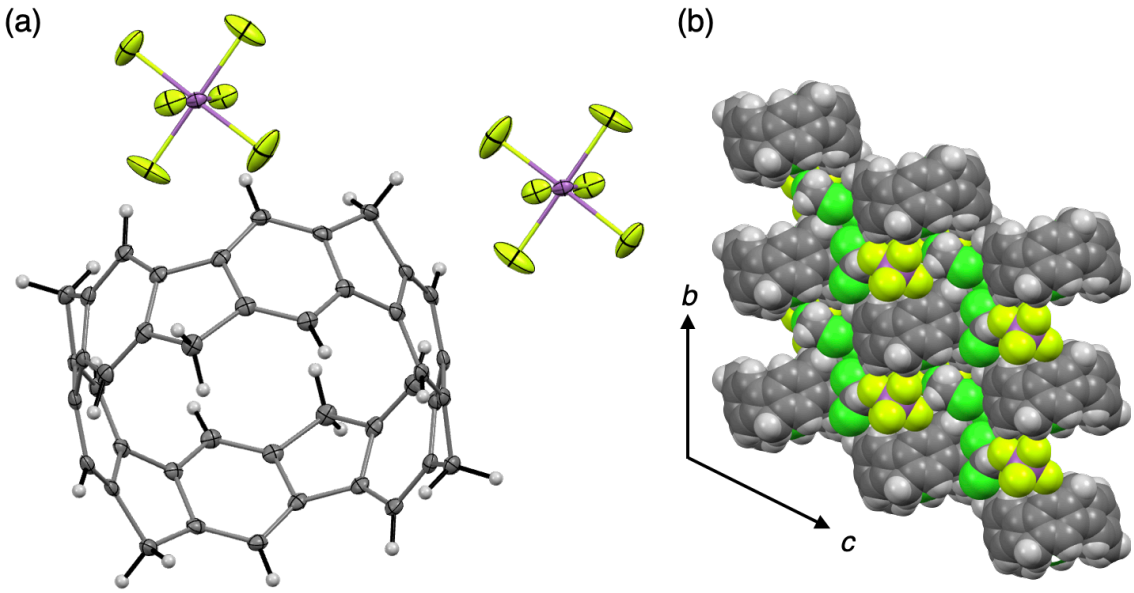

Figure S4. (a) X-ray crystal structures of **2** ([6]MCPP^{2+}(SbF_6^-)$_2$) with solvents omitted for clarity. (b) Packing structures viewed along the *a*-axis.

3. Comparison among [6]MCPP, [6]MCPP^{2+}, [6]CPP^{2+} (regarding Table 1 in the main text)

Table S2. Comparison among [6]MCPP[S8] [6]MCPP^{2+}, [6]CPP^{2+} [S9].

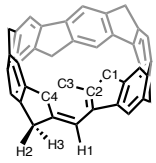

	[6]MCPP	[6]MCPP^{2+}	[6]CPP^{2+}
Diameter [Å]	7.758	7.675	-
C1–C2 [Å]	1.518	1.514	-
C2–C3 [Å]	1.384	1.368	-
C2–C4 [Å]	1.408	1.436	-
C3–C4 [Å]	1.395	1.415	-
C4–C4 [Å]	1.478	1.428	-
HOMO [eV]	–4.40*	–11.38*	–11.62*
LUMO [eV]	–1.74*	–9.47*	–9.79*
Energy gap [eV]	2.66*	1.91*	1.83*
Abs. peak [nm]	347, 370	453, 745	464, 792
Flu. peak [nm]	-	677, 752	801
Fluorescence quantum yield	-	23%	1.8%
NMR (H1) [ppm]	7.88	4.01	5.30
NMR (H2) [ppm]	4.27	3.51	-
NMR (H3) [ppm]	4.01	–0.13	-
NMR (C1) [ppm]	41.2	36.2	-
NMR (C2) [ppm]	149.0	161.2	-
NMR (C3) [ppm]	122.4	123.7	-
NMR (C4) [ppm]	137.7	164.9	-
NICS(belt center)	–1.188**	–19.971**	–18.742**
NICS(-1)	–7.033**	–25.629**	–25.369**
NICS(0)	–5.679**	–9.013**	–8.964**
NICS(1)	–5.384**	–3.595**	–4.131**

*B3LYP/6-31G(d)level **GIAO-B3LYP/6-311+G(2d,p)

4. Photophysical measurements (regarding Figure 3 in the main text)

The measurement of fluorescence for **1** was unsuccessful in spite of our effort. The measurement of fluorescence in IR regions is often difficult, also because of depopulation of the excited state by electronic-vibrational energy transfer (see *e.g.* Monguzzi et al. *New J. Chem.*, **2009**, *33*, 1542–1548). Moreover, according to Kasha rules the fluorescing state should be the S_1 state of symmetry E_u (derived from the $e_u \rightarrow a_{2g}$ single excitation), which can be expected to undergo an efficient non-radiative decay via dynamic Jahn-Teller effect. As a matter of fact, we find in a preliminary calculation that S_1 is second-order saddle and tends to lower symmetry following e_u vibrational modes.

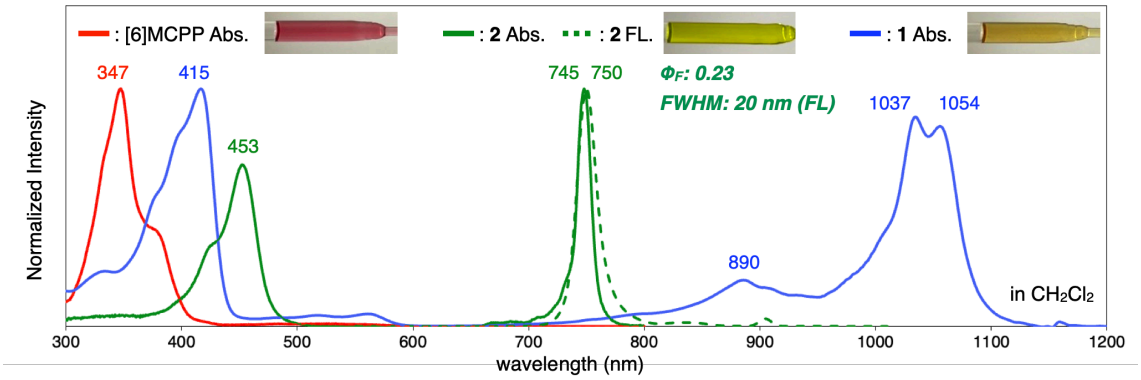

Figure S5. UV–vis–NIR absorption (solid line) and fluorescence (dashed line) spectra of CH_2Cl_2 solutions of [6]MCPP, **1**, and **2**. Fluorescence spectrum of **2** was recorded upon excitation at 450 nm.

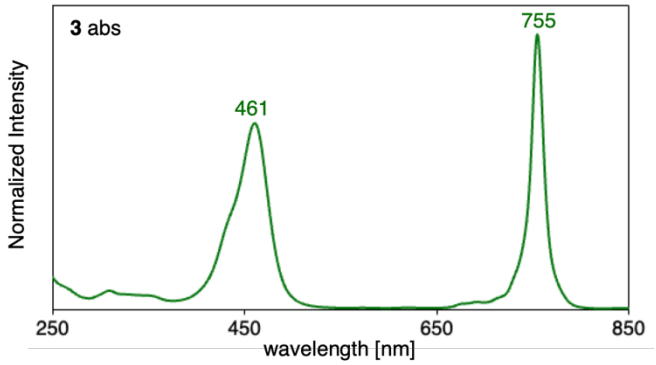

Figure S6. UV–vis–NIR absorption spectra of a CH_2Cl_2 solution of **3**.

5. DFT and TD-DFT calculations

Table S3. Simulated NMR chemical shifts (GIAO-B3LYP/6-311+G(2d,p)).

[6]MCPP^{2+}		NMR chemical shifts [ppm]
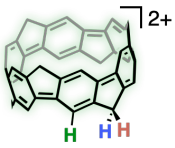	H	4.13
	H	3.92 (outer)
	H	–0.67 (inner)

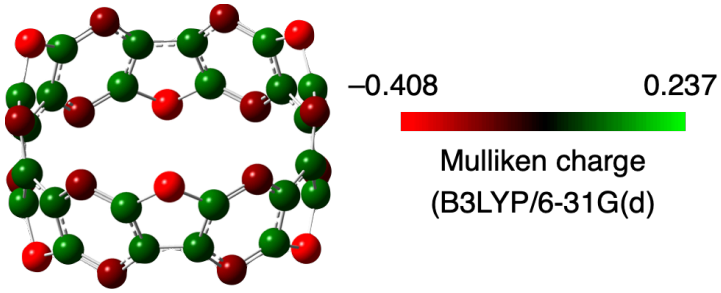

Figure S7. Mulliken charge of [6]MCPP^{2+} (B3LYP/6-31G(d))

Table S4. NICS value of [6]MCPP, [6]MCPP^{2+}, and [6]CPP^{2+} (GIAO-B3LYP/6-311+G(2d,p))

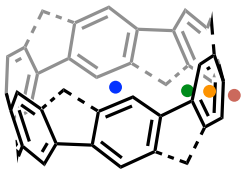

	[6]MCPP	[6]MCPP^{2+}	[6]CPP^{2+}
NICS(belt center)	–1.19	–19.97	–18.74
NICS(-1)	–7.03	–25.63	–25.37
NICS(0)	–5.68	–9.01	–8.96
NICS(1)	–5.38	–3.56	–4.13

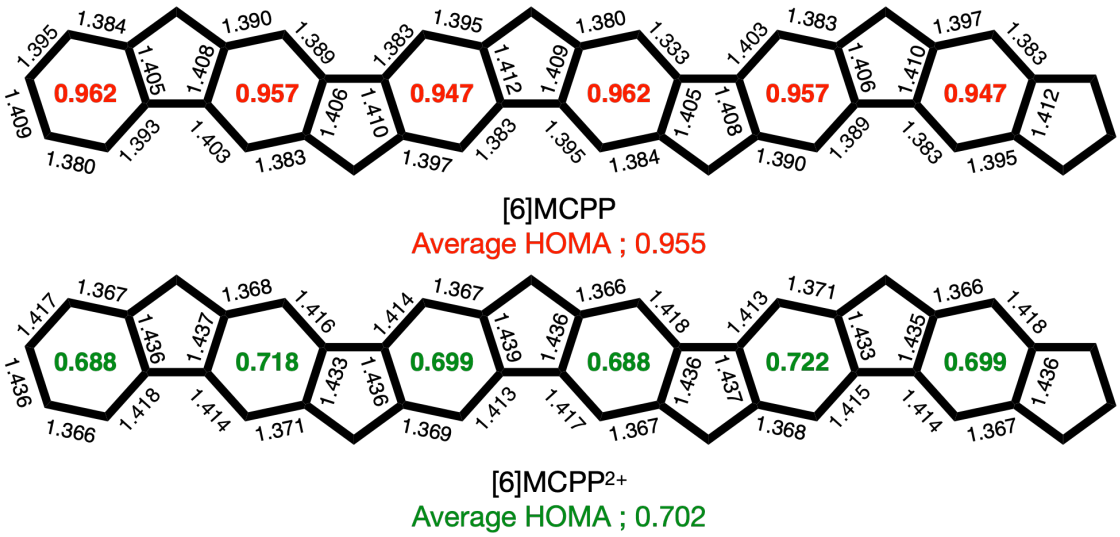

Figure S8. Bond length (Å) and HOMA value of [6]MCPP and [6]MCPP^{2+} (belt structure shown unfolded)

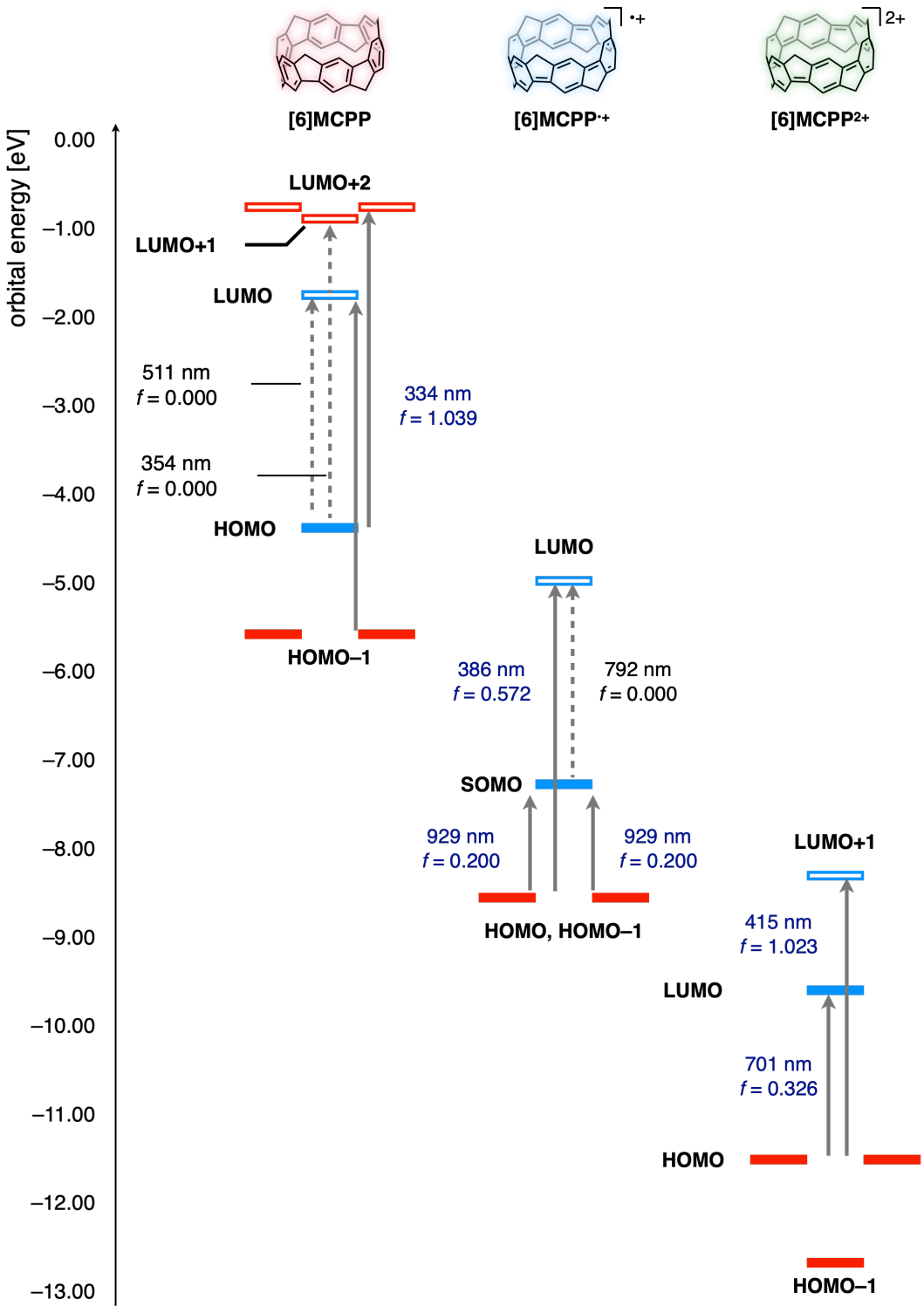

Figure S9. TD-DFT calculations of [6]MCPP, [6]MCPP$^{\bullet+}$ and [6]MCPP^{2+} ((U)B3LYP/6-31G(d)).

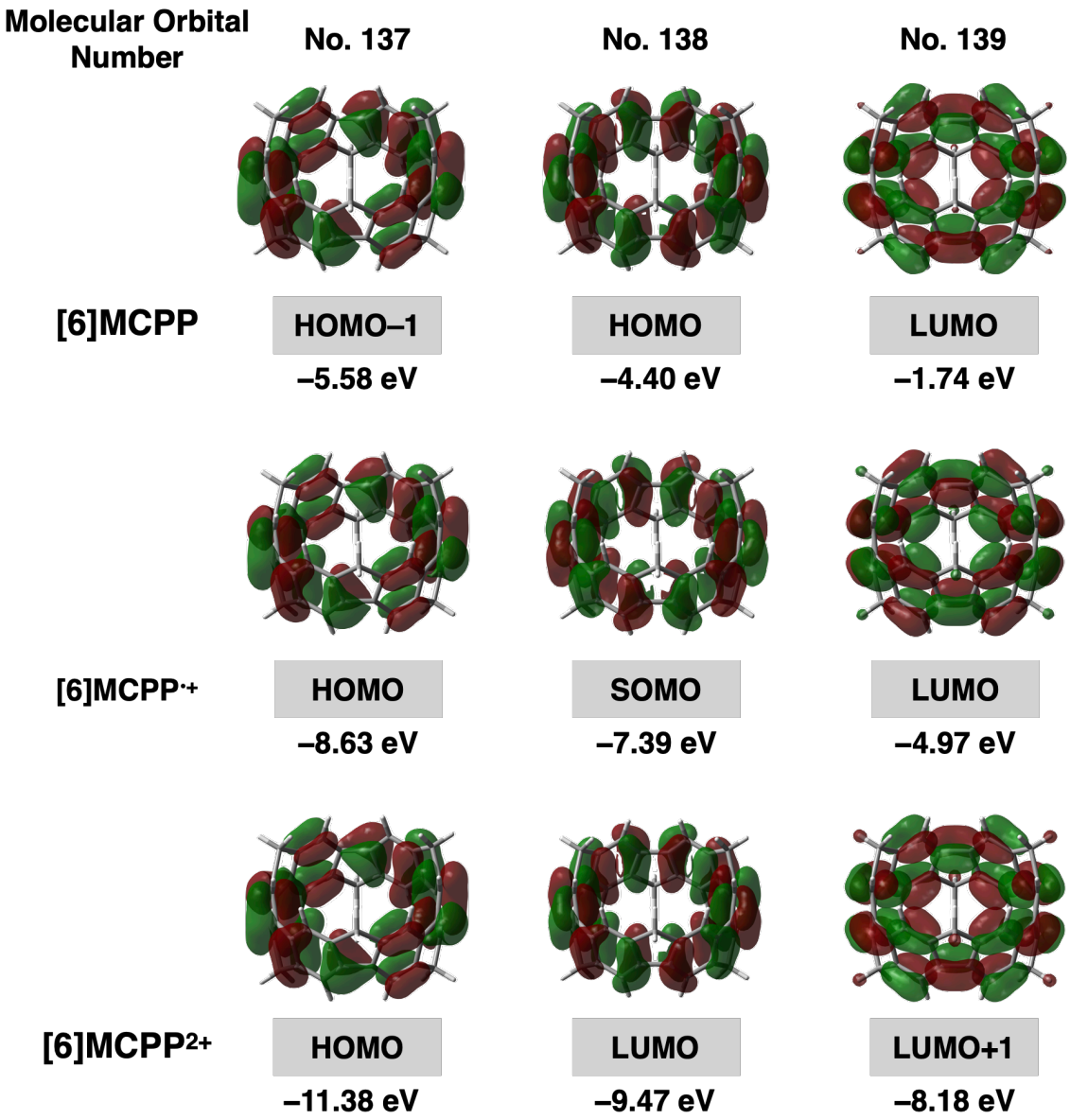

Figure S10. Orbital energies of [6]MCPP, [6]MCPP$^{\cdot+}$ and [6]MCPP^{2+} (B3LYP/6-31G(d)).

In order to reevaluate the origin of the weak absorption (SOMO to LUMO transition) appearing around 890 nm in **1**, 15 different calculations were performed under multiple DFT/TD-DFT conditions. Since long-range-corrected and high-HF exchange-rate functionalities seem to be suitable to describe both electronic states and excited states of radical species, we combined UB3LYP, CAM-B3LYP, M06-2X, PBE0, or ωB97X- D with 6-31+G(d,p) or 6-311++G(d,p). Note that the aug-cc-pVTZ basis, which is expected to give more accurate results, was also investigated. However, the calculation has not been successful probably due to the very high computational cost. Therefore, we verified the oscillator strength of the SOMO to LUMO transition for 10 different calculation results. The results are as follows.

UB3LYP/6-31+G(d,p)

Excited State 1: 2.011-AU 1.3188 eV 940.10 nm f=0.2112 <S**2>=0.761
136B ->139B 0.14122
137B ->138B 0.98254
This state for optimization and/or second-order correction.
Total Energy, E(TD-HF/TD-DFT) = -1614.74188871
Copying the excited state density for this state as the 1-particle RhoCI density.

Excited State 2: 2.011-AU 1.3191 eV 939.91 nm f=0.2109 <S**2>=0.761
136B ->138B 0.98254
137B ->139B -0.14123

Excited State 3: 2.098-AG 1.5212 eV 815.05 nm **f=0.0000** <S**2>=0.851
136A ->141A 0.11526
137A ->140A -0.11535
138A ->139A 0.97534

Excited State 4: 2.022-AU 2.2637 eV 547.70 nm f=0.0000 <S**2>=0.772
135B ->138B 0.99517

UB3LYP/6-311++G(d,p)

Excited State 1: 2.011-AU 1.3326 eV 930.42 nm f=0.2073 <S**2>=0.761
136B -> 139B -0.14293
137B -> 138B 0.98210
This state for optimization and/or second-order correction.
Total Energy, E(TD-HF/TD-DFT) = -1615.02243305
Copying the excited state density for this state as the 1-particle RhoCI density.

Excited State 2: 2.011-AU 1.3329 eV 930.19 nm f=0.2070 <S**2>=0.761
136B -> 138B 0.98209
137B -> 139B 0.14295

Excited State 3: 2.092-AG 1.5054 eV 823.58 nm **f=0.0000** <S**2>=0.844
136A -> 141A -0.11228
137A -> 140A 0.11238
138A -> 139A 0.97705

Excited State 4: 2.022-AU 2.2763 eV 544.67 nm f=0.0000 <S**2>=0.772
135B -> 138B 0.99521

CAM-B3LYP/6-31+G(d,p)

Excited State 1: 2.065-AU 0.9790 eV 1266.49 nm f=0.2621 <S**2>=0.816
136B ->139B 0.24808
137B ->138B 0.99602
136B <-139B 0.18817
137B <-138B 0.20919

This state for optimization and/or second-order correction.
Total Energy, E(TD-HF/TD-DFT) = -1613.81408401
Copying the excited state density for this state as the 1-particle RhoCI density.

Excited State 2: 2.065-AU 0.9794 eV 1265.86 nm f=0.2617 <S**2>=0.816
136B ->138B 0.99598
137B ->139B -0.24815
136B <-138B 0.20907
137B <-139B -0.18818

Excited State 3: 2.361-AG 1.8004 eV 688.66 nm **f=0.0000** <S**2>=1.144
136A ->141A -0.24767
137A ->140A 0.24787
138A ->139A 0.89415
136B ->142B 0.12631
137B ->141B -0.12644

Excited State 4: 3.166-AU 2.3471 eV 528.23 nm f=0.0000 <S**2>=2.257
137A ->139A -0.42853
138A ->140A -0.44645
128B ->141B 0.10398
129B ->142B 0.10395
136B ->138B 0.16876
137B ->139B 0.67761

CAM-B3LYP/6-311++G(d,p)
Excited State 1: 2.066-AU 0.9984 eV 1241.89 nm f=0.2562 <S**2>=0.817
136B -> 139B -0.25110
137B -> 138B 0.99484
136B <- 139B -0.18787
137B <- 138B 0.20740
This state for optimization and/or second-order correction.
Total Energy, E(TD-HF/TD-DFT) = -1614.09974294
Copying the excited state density for this state as the 1-particle RhoCI density.

Excited State 2: 2.066-AU 0.9989 eV 1241.24 nm f=0.2558 <S**2>=0.817
136B -> 138B 0.99479
137B -> 139B 0.25118
136B <- 138B 0.20728
137B <- 139B 0.18787

Excited State 3: 2.342-AG 1.7866 eV 693.97 nm **f=0.0000** <S**2>=1.121
136A -> 141A -0.24344
137A -> 140A 0.24365
138A -> 139A 0.90062
136B -> 142B 0.12084

137B -> 141B -0.12096

Excited State 4: 3.164-AU 2.3525 eV 527.03 nm f=0.0000 <S**2>=2.253
137A -> 139A -0.42835
138A -> 140A -0.44625
128B -> 141B 0.10250
129B -> 142B 0.10246
136B -> 138B -0.17011
137B -> 139B 0.68318

M06-2X/6-31+G(d,p)

Excited State 1: 2.019-AU 1.1600 eV 1068.82 nm f=0.2555 <S**2>=0.769
136B ->139B -0.17391
137B ->138B 0.99250
136B <-139B -0.13980
137B <-138B 0.11797
This state for optimization and/or second-order correction.
Total Energy, E(TD-HF/TD-DFT) = -1614.07895124
Copying the excited state density for this state as the 1-particle RhoCI density.

Excited State 2: 2.019-AU 1.1602 eV 1068.69 nm f=0.2551 <S**2>=0.769
136B ->138B 0.99249
137B ->139B 0.17391
136B <-138B 0.11796
137B <-139B 0.13980

Excited State 3: 2.174-AG 1.9564 eV 633.75 nm **f=0.0000** <S**2>=0.931
136A ->141A -0.19296
137A ->140A 0.19310
138A ->139A 0.94838

Excited State 4: 3.170-AU 2.6232 eV 472.65 nm f=0.0003 <S**2>=2.263
137A ->139A -0.40897
138A ->140A -0.42536
137B ->139B 0.76280

M06-2X/6-311++G(d,p)

Excited State 1: 2.020-AU 1.1699 eV 1059.76 nm f=0.2505 <S**2>=0.770
136B -> 139B -0.17890
137B -> 138B 0.99193
136B <- 139B -0.14126
137B <- 138B 0.12042
This state for optimization and/or second-order correction.
Total Energy, E(TD-HF/TD-DFT) = -1614.38670142
Copying the excited state density for this state as the 1-particle RhoCI density.

Excited State 2: 2.020-AU 1.1704 eV 1059.33 nm f=0.2500 <S**2>=0.770
136B -> 138B 0.99192
137B -> 139B 0.17894
136B <- 138B 0.12037
137B <- 139B 0.14127

Excited State 3: 2.173-AG 1.9164 eV 646.97 nm **f=0.0000** <S**2>=0.930
136A -> 141A -0.19236
137A -> 140A 0.19255
138A -> 139A 0.94875

Excited State 4: 3.169-AU 2.6016 eV 476.56 nm f=0.0002 <S**2>=2.260
137A -> 139A -0.41182
138A -> 140A -0.42893
137B -> 139B 0.75834

PBE0/6-31+G(d,p)

Excited State 1: 2.022-AU 1.3171 eV 941.37 nm f=0.2260 <S**2>=0.772
136B ->139B -0.16033
137B ->138B 0.98154
This state for optimization and/or second-order correction.
Total Energy, E(TD-HF/TD-DFT) = -1612.88700449
Copying the excited state density for this state as the 1-particle RhoCI density.

Excited State 2: 2.022-AU 1.3173 eV 941.20 nm f=0.2257 <S**2>=0.772
136B ->138B 0.98154
137B ->139B 0.16035

Excited State 3: 2.150-AG 1.5564 eV 796.62 nm **f=0.0000** <S**2>=0.905
136A ->141A -0.14198
137A ->140A 0.14208
138A ->139A 0.96178

Excited State 4: 3.154-AU 2.3133 eV 535.96 nm f=0.0029 <S**2>=2.236
137A ->139A -0.43780
138A ->140A -0.46519
137B ->139B 0.70484

PBE0/6-311++G(d,p)

Excited State 1: 2.022-AU 1.3304 eV 931.90 nm f=0.2220 <S**2>=0.772
136B -> 139B -0.16260
137B -> 138B 0.98110
This state for optimization and/or second-order correction.
Total Energy, E(TD-HF/TD-DFT) = -1613.14475326
Copying the excited state density for this state as the 1-particle RhoCI density.

Excited State 2: 2.022-AU 1.3308 eV 931.66 nm f=0.2217 <S**2>=0.772
136B -> 138B 0.98109
137B -> 139B 0.16263

Excited State 3: 2.141-AG 1.5405 eV 804.83 nm **f=0.0000** <S**2>=0.895
136A -> 141A -0.13855
137A -> 140A 0.13867
138A -> 139A 0.96434

Excited State 4: 3.153-AU 2.3165 eV 535.23 nm f=0.0025 <S**2>=2.235
137A -> 139A -0.43722
138A -> 140A -0.46411
137B -> 139B 0.70926

ω B97X-D/6-31+G(d,p)

Excited State 1: 2.065-A 0.9025 eV 1373.81 nm f=0.2587 <S**2>=0.816
136B ->138B 1.00816
137B ->139B 0.25636
136B <-138B 0.27274
137B <-139B 0.19895
This state for optimization and/or second-order correction.
Total Energy, E(TD-HF/TD-DFT) = -1614.21238351
Copying the excited state density for this state as the 1-particle RhoCI density.

Excited State 2: 2.056-A 1.0430 eV 1188.71 nm f=0.2607 <S**2>=0.806
136B ->139B -0.20958
137B ->138B 1.00176
136B <-139B -0.17569
137B <-138B 0.21735

Excited State 3: 2.439-A 1.9294 eV 642.59 nm **f=0.0065** <S**2>=1.237
136A ->140A 0.25195
137A ->141A 0.26671
138A ->139A 0.87635
136B ->141B 0.11818
137B ->142B -0.12080

Excited State 4: 3.098-A 2.4432 eV 507.47 nm f=0.0000 <S**2>=2.150
136A ->139A -0.42306
138A ->139A 0.12214
138A ->140A -0.40941
138A ->142A -0.12205
128B ->141B 0.10787
129B ->142B 0.10198
133B ->138B 0.11334
136B ->138B -0.14562

137B ->139B 0.66169
137B ->142B 0.11064

ω B97X-D/6-311++G(d,p)

Excited State 1: 2.067-A 0.9135 eV 1357.29 nm f=0.2530 <S**2>=0.818
136B -> 138B 1.00753
137B -> 139B 0.26126
136B <- 138B 0.27319
137B <- 139B 0.20107
This state for optimization and/or second-order correction.
Total Energy, E(TD-HF/TD-DFT) = -1614.48114555
Copying the excited state density for this state as the 1-particle RhoCI density.

Excited State 2: 2.057-A 1.0465 eV 1184.78 nm f=0.2557 <S**2>=0.808
136B -> 139B -0.21669
137B -> 138B 1.00167
136B <- 139B -0.17876
137B <- 138B 0.22106

Excited State 3: 2.417-A 1.9126 eV 648.24 nm **f=0.0060** <S**2>=1.210
136A -> 140A 0.24790
137A -> 141A 0.26351
138A -> 139A 0.88302
136B -> 142B -0.11429
137B -> 141B 0.11711

Excited State 4: 3.114-A 2.4413 eV 507.87 nm f=0.0000 <S**2>=2.174
136A -> 139A -0.42443
138A -> 139A 0.11212
138A -> 140A -0.40945
138A -> 142A 0.13298
136B -> 138B -0.15221
137B -> 139B 0.67106
137B -> 141B -0.10741

Based on these calculations, the SOMO (138) → LUMO (139) did not clearly appear as a transition with large contribution. This result might indicate a limitation of the (TD)DFT calculation, particularly the inability of the standard TD-DFT with the linear response method to adequately reproduce the subtle oscillator strengths of the electronic states and forbidden transitions of radical species with complicated properties. We think it would be necessary to investigate more sophisticated methods and corrections with vibration effects for further discussion with experimental results.

Belt current effect on the ^{13}C NMR signals

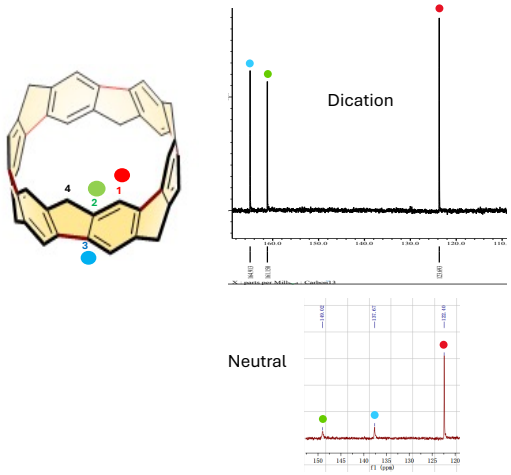

Table S5. [6]MCPP dication - calculated ^{13}C NMR chemical shifts for the free molecule in ppm, reference TMS. AvAD=Averaged Absolute Deviations with respect to expermental results: 123.69 C1, 161.15 C2, 164.91 C3, and 36.25 C4.

Functional	CSGT					GIAO				
	C1	C2	C3	C4	AvAD	C1	C2	C3	C4	AvAD
B3LYP	126.08	169.15	171.17	40.83	5.31	126.28	169.98	171.95	41.66	5.97
B97-2	122.42	163.55	165.48	39.56	1.89	122.12	164.13	166.01	40.18	2.39
BHandHLYP	127.05	170.77	173.12	37.96	5.72	127.10	171.35	173.68	38.51	6.16

Table S6. [6]MCPP dication in CD_2Cl_2, see Table S5 for other details.

Functional	CSGT					GIAO				
	C1	C2	C3	C4	AvAD	C1	C2	C3	C4	AvAD
B3LYP	127.82	169.71	172.59	41.07	6.30	128.06	170.52	173.37	41.90	6.96
B972	124.14	164.17	166.92	39.82	2.26	124.15	164.67	167.36	40.40	2.65
BHandHLYP	128.73	171.46	174.60	38.22	6.75	128.65	171.95	175.17	38.70	7.12

Table S7. [6]MCPP neutral for the free molecule, see Table S5 for other details.

Functional	CSGT					GIAO				
	C1	C2	C3	C4	AvAD	C1	C2	C3	C4	AvAD
B3LYP	124.94	155.08	141.67	44.75	4.04	125.21	156.04	142.57	45.52	4.76
B97-2	122.07	150.16	137.36	43.51	1.02	121.68	150.87	138.04	44.09	1.46
BHandHLYP	126.85	156.24	144.42	42.46	4.92	126.87	156.94	145.11	43.03	5.41

Table S8. [6]MCPP neutral in CD_2Cl_2, see Table S5 for other details.

Functional	CSGT					GIAO				
	C1	C2	C3	C4	AvAD	C1	C2	C3	C4	AvAD
B3LYP	125.99	156.52	142.28	45.06	4.89	126.28	157.37	142.80	46.00	5.54
B97-2	123.12	151.58	137.91	43.81	1.53	123.06	152.22	138.48	44.33	1.95
BHandHLYP	127.91	157.62	144.96	42.73	5.73	127.93	158.23	145.55	43.22	6.16

Both molecules belong to the D_{3d} point group symmetry and display four signals in the decoupled ^{13}C NMR spectra. These have been arbitrarily numerated as shown in the figure. A color has been attached to them: red C1, green C2, blue C3, and black C4.

Signal assignment is trivial for C1 and C4. The assignment of C2 and C3 can be made based on the calculation results. This is indicated by the small colored dots reported in the NMR spectra above. The NMR spectrum of the neutral species is from the supplementary information by Kono et al. *J. Am. Chem. Soc.* **2023**, *145*, 8939−8946. C4 is not shown.

The calculations were carried out using the 6-311+G(2d,p) basis set. Three functionals were adopted: B3LYP, B97-2, and BHandHLYP. Molecular geometries for neutral and dication, as well as TMS, were optimized at the same level of accuracy adopted for the NMR calculations. Chemical shifts were obtained for CSGT and GIAO methods for the free molecules and including solvent effect (dichloromethane).

Calculated chemical shifts are reported in four table. Table 1 for dication no solvent effects (free); Table 2 for dication in dichloromethane; Table 3 neutral free; Table 4 neutral in dichloromethane. In each table, the three functionals can be compared for CSGT e GIAO. To facilitate ranking the absolute deviation from experimental chemical shifts averaged over the four carbons is also reported under the heading AvAD. Without exceptions the combination B97-2/CSGT provides the smaller AvAD (best matching). The results are better for the free molecule with respect to the inclusion of the solvent effects. Remarkably, it turns out that CSGT is always a little better than GIAO.

The interesting fact is that, changing the oxidation state, two of the experimental carbon signals, namely C2 and C3, move considerably downfield (C2 by ~12 ppm and C3 by ~27 ppm); that of C4 moves ~5 ppm upfield; C1 signal changes very little remaining within the aromatic region. Theoretical results (see Table 1 and 3) reproduce the experimental shifts nicely.

Consequently, it seems quite likely that C2, C3, C4 shifts are related to the reversal of the belt current. To see whether this is the case, we considered the feature of the CSGT method of dissecting the induced current and related magnetic properties into orbital contributions and performed the following theoretical experiment. Since, in both molecules, the belt currents are induced by a magnetic field parallel to the main symmetry axis and are almost completely due to virtual transitions from the frontier orbitals, we have calculated the contributions to the parallel component of the magnetic shielding $\sigma_{\parallel}^{\mathrm{N}}(\mathrm{MFO})$ at each Nucleus (N) of interest due to the Molecular Frontier Orbitals (MFO). Then, we have taken the difference $\sigma_{\parallel}^{\mathrm{N}}(\mathrm{dication}) - \sigma_{\parallel}^{\mathrm{N}}(\mathrm{neutral})$, for N=C2, C3, and C4 (also H_{in}, H_{out}, and H_{ar}) changed the sign (from shielding to chemical shift) and divided by three (weight to average) to obtain the contributions to the relative chemical shifts. Results are shown in Table S9.

Table S9. Predicted change of the NMR chemical shifts due to the belt current.

N	$\sigma_{\parallel}^{\mathrm{N}}(\mathrm{MFO})$		Relative shifts	
	dication	neutral	Theor.	Expt.
H_{in}	13.27	-3.35	-5.54	-4.31
H_{out}	1.51	-0.38	-0.63	-0.62
H_{ar}	11.32	-2.74	-4.69	-3.67
C2	**-13.34**	**6.41**	**6.58**	**12.13**
C3	**-33.33**	**17.04**	**16.79**	**27.24**
C4	**6.74**	**-2.52**	**-3.09**	**-4.95**

As can be observed, the agreement between theoretical estimates and experimental relative shifts is encouraging, especially for the proton. For ^{13}C some other contribution is evidently necessary, but it is interesting to observe the concordance of the shift (down or up field) and the relative magnitude which are proportionate to the experimental ones.

Table S10. Cartesian coordinates of optimized structure of [6]MCPP^{2+} in S_0.

C	-3.927363	-0.433079	1.373436	C	-1.588624	-3.617736	-1.373436
C	-3.927363	0.433079	-1.373436	C	-2.733225	-2.918795	-1.066388
C	-3.766034	1.345486	-0.298062	C	-3.048242	-2.588738	0.298062
C	-3.894363	0.907645	1.066388	C	-2.338739	-3.184657	1.373436
C	-3.048242	2.588738	-0.298062	C	-1.161138	-3.826440	1.066388
C	-2.338739	3.184657	-1.373436	C	0.000000	-4.137827	1.992961
C	-1.161138	3.826440	-1.066388	C	-3.583464	-2.068914	-1.992961
C	-0.717792	3.934224	0.298062	C	-3.766034	-1.345486	0.298062
C	-1.588624	3.617736	1.373436	C	-3.894363	-0.907645	-1.066388
C	-2.733225	2.918795	1.066388	H	-3.888407	-0.771182	2.404682
C	-3.583464	2.068914	1.992961	H	-3.888407	0.771182	-2.404682
C	0.000000	4.137827	-1.992961	H	-2.612066	2.981868	-2.404682
C	1.588624	3.617736	1.373436	H	-1.276340	3.753050	2.404682
C	0.717792	3.934224	0.298062	H	-4.499631	2.597863	2.291710
C	1.161138	3.826440	-1.066388	H	-3.064720	1.769417	2.907575
C	2.338739	3.184657	-1.373436	H	0.000000	3.538834	-2.907575
C	3.048242	2.588738	-0.298062	H	0.000000	5.195726	-2.291710
C	2.733225	2.918795	1.066388	H	1.276340	3.753050	2.404682
C	3.766034	1.345486	-0.298062	H	2.612066	2.981868	-2.404682
C	3.927363	0.433079	-1.373436	H	3.888407	0.771182	-2.404682
C	3.894363	-0.907645	-1.066388	H	3.888407	-0.771182	2.404682
C	3.766034	-1.345486	0.298062	H	4.499631	2.597863	2.291710
C	3.927363	-0.433079	1.373436	H	3.064720	1.769417	2.907575
C	3.894363	0.907645	1.066388	H	3.064720	-1.769417	-2.907575
C	3.583464	2.068914	1.992961	H	4.499631	-2.597863	-2.291710
C	3.583464	-2.068914	-1.992961	H	2.612066	-2.981868	2.404682
C	2.338739	-3.184657	1.373436	H	1.276340	-3.753050	-2.404682
C	3.048242	-2.588738	0.298062	H	-1.276340	-3.753050	-2.404682
C	2.733225	-2.918795	-1.066388	H	-2.612066	-2.981868	2.404682
C	1.588624	-3.617736	-1.373436	H	0.000000	-5.195726	2.291710
C	0.717792	-3.934224	-0.298062	H	0.000000	-3.538834	2.907575
C	1.161138	-3.826440	1.066388	H	-3.064720	-1.769417	-2.907575
C	-0.717792	-3.934224	-0.298062	H	-4.499631	-2.597863	-2.291710

Table S11. Cartesian coordinates of optimized structure of [6]MCPP in S_0.

C	-3.959872	-0.443140	1.350744	C	-1.596166	-3.650920	-1.350744
C	-3.959872	0.443140	-1.350744	C	-2.755141	-2.944057	-1.046616
C	-3.831978	1.358926	-0.293764	C	-3.092854	-2.639127	0.293764
C	-3.927199	0.913993	1.046616	C	-2.363706	-3.207780	1.350744
C	-3.092854	2.639127	-0.293764	C	-1.172058	-3.858051	1.046616
C	-2.363706	3.207780	-1.350744	C	0.000000	-4.101438	1.985672
C	-1.172058	3.858051	-1.046616	C	-3.551950	-2.050719	-1.985672
C	-0.739125	3.998054	0.293764	C	-3.831978	-1.358926	0.293764
C	-1.596166	3.650920	1.350744	C	-3.927199	-0.913993	-1.046616
C	-2.755141	2.944057	1.046616	H	-3.868157	-0.770805	2.383887
C	-3.551950	2.050719	1.985672	H	-3.868157	0.770805	-2.383887
C	0.000000	4.101438	-1.985672	H	-2.601615	2.964520	-2.383887
C	1.596166	3.650920	1.350744	H	-1.266542	3.735325	2.383887
C	0.739125	3.998054	0.293764	H	-4.442403	2.564822	2.378107
C	1.172058	3.858051	-1.046616	H	-2.968498	1.713863	2.849209
C	2.363706	3.207780	-1.350744	H	0.000000	3.427726	-2.849209
C	3.092854	2.639127	-0.293764	H	0.000000	5.129645	-2.378107
C	2.755141	2.944057	1.046616	H	1.266542	3.735325	2.383887
C	3.831978	1.358926	-0.293764	H	2.601615	2.964520	-2.383887
C	3.959872	0.443140	-1.350744	H	3.868157	0.770805	-2.383887
C	3.927199	-0.913993	-1.046616	H	3.868157	-0.770805	2.383887
C	3.831978	-1.358926	0.293764	H	4.442403	2.564822	2.378107
C	3.959872	-0.443140	1.350744	H	2.968498	1.713863	2.849209
C	3.927199	0.913993	1.046616	H	2.968498	-1.713863	-2.849209
C	3.551950	2.050719	1.985672	H	4.442403	-2.564822	-2.378107
C	3.551950	-2.050719	-1.985672	H	2.601615	-2.964520	2.383887
C	2.363706	-3.207780	1.350744	H	1.266542	-3.735325	-2.383887
C	3.092854	-2.639127	0.293764	H	-1.266542	-3.735325	-2.383887
C	2.755141	-2.944057	-1.046616	H	-2.601615	-2.964520	2.383887
C	1.596166	-3.650920	-1.350744	H	0.000000	-5.129645	2.378107
C	0.739125	-3.998054	-0.293764	H	0.000000	-3.427726	2.849209
C	1.172058	-3.858051	1.046616	H	-2.968498	-1.713863	-2.849209
C	-0.739125	-3.998054	-0.293764	H	-4.442403	-2.564822	-2.378107

Table S12. Cartesian coordinates of optimized structure of [6]CPP^{2+} in S_0.

C	4.156120	0.354290	1.210323	C	1.713879	-3.782190	0.000013
C	4.132728	-0.406913	-0.000015	C	2.384662	-3.421724	1.210396
C	4.155919	0.354240	-1.210388	C	3.367056	-2.461438	1.210399
C	3.815318	1.685122	-1.210390	C	3.742710	-1.799035	0.000016
C	3.429352	2.341570	-0.000016	C	3.367188	-2.461571	-1.210337
C	3.815521	1.685172	1.210324	C	2.384791	-3.421851	-1.210338
C	1.771084	3.775957	1.210394	H	4.334108	-0.133406	2.161798
C	2.418670	3.375304	0.000014	H	4.333689	-0.133507	-2.161876
C	1.771135	3.776142	-1.210334	H	3.736877	2.198288	-2.161885
C	0.448276	4.146666	-1.210336	H	3.737300	2.198400	2.161805
C	-0.313256	4.140540	0.000013	H	2.282356	3.685952	2.161887
C	0.448224	4.146486	1.210394	H	2.282469	3.686338	-2.161815
C	-1.713878	3.782191	-0.000014	H	-0.035269	4.335624	-2.161813
C	-2.384787	3.421852	1.210338	H	-0.035371	4.335257	2.161882
C	-3.367185	2.461571	1.210340	H	-2.051343	3.819769	2.161815
C	-3.742711	1.799036	-0.000012	H	-3.772568	2.137256	2.161828
C	-3.367060	2.461438	-1.210396	H	-3.772299	2.136978	-2.161896
C	-2.384665	3.421724	-1.210396	H	-2.051090	3.819503	-2.161884
C	-4.132729	0.406913	0.000019	H	-4.333687	0.133504	2.161881
C	-4.155918	-0.354242	1.210391	H	-3.736875	-2.198291	2.161886
C	-3.815317	-1.685124	1.210392	H	-3.737303	-2.198398	-2.161805
C	-3.429352	-2.341571	0.000016	H	-4.334112	0.133409	-2.161794
C	-3.815523	-1.685171	-1.210323	H	-2.282355	-3.685946	-2.161890
C	-4.156123	-0.354289	-1.210319	H	0.035373	-4.335251	-2.161886
C	-2.418670	-3.375305	-0.000016	H	0.035270	-4.335630	2.161809
C	-1.771083	-3.775954	-1.210398	H	-2.282469	-3.686345	2.161811
C	-0.448223	-4.146482	-1.210398	H	2.051084	-3.819503	2.161883
C	0.313257	-4.140540	-0.000016	H	3.772292	-2.136977	2.161900
C	-0.448276	-4.146669	1.210332	H	3.772574	-2.137255	-2.161824
C	-1.771135	-3.776146	1.210331	H	2.051349	-3.819769	-2.161815

Table S13. Cartesian coordinates of optimized structure of [6]MCPP$^{\bullet+}$ in S_0.

C	3.633077	-1.590825	1.361586	C	3.194233	2.350924	-1.361586
C	3.194498	-2.351078	-1.361528	C	3.840049	1.166244	-1.056441
C	2.613637	-3.070214	-0.295258	C	3.965702	0.728370	0.295258
C	2.930021	-2.742458	1.056441	C	3.633342	1.590978	1.361528
C	1.352094	-3.798578	-0.295303	C	2.930177	2.742548	1.056400
C	0.438844	-3.941749	-1.361586	C	2.058263	3.564942	1.990236
C	-0.910027	-3.908702	-1.056441	C	4.116462	-0.000037	-1.990236
C	-1.352064	-3.798583	0.295258	C	3.965712	-0.728341	0.295303
C	-0.438844	-3.942056	1.361528	C	3.840205	-1.166333	-1.056400
C	0.910028	-3.908881	1.056400	H	3.742013	-1.268998	2.393727
C	2.058199	-3.564979	1.990236	H	2.970311	-2.606345	-2.393676
C	-2.058263	-3.564942	-1.990236	H	0.772021	-3.875177	-2.393727
C	-3.194233	-2.350924	1.361586	H	-0.772005	-3.875537	2.393676
C	-2.613618	-3.070236	0.295303	H	2.579890	-4.468378	2.337464
C	-2.930177	-2.742548	-1.056400	H	1.738929	-3.012069	2.878863
C	-3.633342	-1.590978	-1.361528	H	-1.739064	-3.011992	-2.878863
C	-3.965702	-0.728370	-0.295258	H	-2.579784	-4.468439	-2.337464
C	-3.840049	-1.166244	1.056441	H	-2.969991	-2.606179	2.393727
C	-3.965712	0.728341	-0.295303	H	-3.742316	-1.269193	-2.393676
C	-3.633077	1.590825	-1.361586	H	-3.742013	1.268998	-2.393727
C	-2.930021	2.742458	-1.056441	H	-2.970311	2.606345	2.393676
C	-2.613637	3.070214	0.295258	H	-5.159674	-0.000061	2.337464
C	-3.194498	2.351078	1.361528	H	-3.477993	0.000078	2.878863
C	-3.840205	1.166333	1.056400	H	-1.738929	3.012069	-2.878863
C	-4.116462	0.000037	1.990236	H	-2.579890	4.468378	-2.337464
C	-2.058199	3.564979	-1.990236	H	-0.772021	3.875177	2.393727
C	-0.438844	3.941749	1.361586	H	0.772005	3.875537	-2.393676
C	-1.352094	3.798578	0.295303	H	2.969991	2.606179	-2.393727
C	-0.910028	3.908881	-1.056400	H	3.742316	1.269193	2.393676
C	0.438844	3.942056	-1.361528	H	2.579784	4.468439	2.337464
C	1.352064	3.798583	-0.295258	H	1.739064	3.011992	2.878863
C	0.910027	3.908702	1.056441	H	3.477993	-0.000078	-2.878863
C	2.613618	3.070236	-0.295303	H	5.159674	0.000061	-2.337464

Table S14. Cartesian coordinates of optimized structure of [6]CPP$^{\bullet+}$ in S_0.

C	-0.011978	-3.974585	-1.254277	C	3.916985	-1.449117	0.040382
C	0.703359	-4.115980	-0.040020	C	3.737128	-2.252632	-1.117408
C	-0.082432	-4.362301	1.117718	C	2.845051	-3.308111	-1.117347
C	-1.442624	-4.117853	1.117657	C	2.082859	-3.619383	0.040510
C	-2.093380	-3.613286	-0.040134	C	2.544231	-3.054674	1.254752
C	-1.373434	-3.729803	-1.254331	C	3.437127	-1.998128	1.254681
C	-3.819756	-2.110027	-1.117376	H	0.522875	-3.881411	-2.192882
C	-3.213530	-2.667282	0.040429	H	0.394724	-4.653505	2.048188
C	-3.449126	-1.977131	1.254659	H	-1.991384	-4.224602	2.048099
C	-3.917892	-0.675665	1.254564	H	-1.842207	-3.456232	-2.193001
C	-4.176499	0.006086	0.040255	H	-3.833436	-2.668955	-2.047779
C	-4.288089	-0.809836	-1.117467	H	-3.101388	-2.393744	2.193404
C	-3.916985	1.449116	-0.040386	H	-3.915717	-0.132888	2.193237
C	-3.437124	1.998126	-1.254685	H	-4.655008	-0.388104	-2.047926
C	-2.544229	3.054671	-1.254757	H	-3.624160	1.488611	-2.193364
C	-2.082859	3.619383	-0.040515	H	-2.073099	3.324024	-2.193477
C	-2.845054	3.308114	1.117341	H	-2.662837	3.836550	2.047825
C	-3.737131	2.252635	1.117402	H	-4.227772	1.984954	2.047919
C	-0.703359	4.115980	0.040018	H	-0.394718	4.653507	-2.048188
C	0.082435	4.362301	-1.117717	H	1.991390	4.224603	-2.048094
C	1.442627	4.117854	-1.117652	H	1.842201	3.456230	2.193006
C	2.093380	3.613286	0.040139	H	-0.522881	3.881410	2.192880
C	1.373431	3.729801	1.254334	H	3.833434	2.668949	2.047785
C	0.011975	3.974585	1.254277	H	4.655006	0.388098	2.047927
C	3.213530	2.667282	-0.040423	H	3.915718	0.132893	-2.193237
C	3.819755	2.110024	1.117381	H	3.101390	2.393750	-2.193399
C	4.288089	0.809833	1.117468	H	4.227768	-1.984949	-2.047925
C	4.176499	-0.006086	-0.040256	H	2.662833	-3.836546	-2.047831
C	3.917892	0.675669	-1.254563	H	2.073104	-3.324029	2.193472
C	3.449127	1.977134	-1.254655	H	3.624164	-1.488616	2.193361

Table S15. Cartesian coordinates of optimized structure of [6]MCPP^{2+} in S_0. (CAM-B3LYP/6-31+G(d,p)).

C	-1.369692	0.435172	3.898534	C	1.370236	3.600151	1.574123
C	1.369692	-0.435172	3.898534	C	1.067227	2.904007	2.713773
C	0.291915	-1.339286	3.743448	C	-0.291751	2.576794	3.031415
C	-1.066940	-0.899975	3.867342	C	-1.369374	3.165286	2.327337
C	0.291751	-2.576794	3.031415	C	-1.066365	3.807050	1.156123
C	1.369374	-3.165286	2.327337	C	-1.992464	4.106264	0.000000
C	1.066365	-3.807050	1.156123	C	1.993543	2.050090	3.548070
C	-0.292551	-3.918657	0.713824	C	-0.291915	1.339286	3.743448
C	-1.370236	-3.600151	1.574123	C	1.066940	0.899975	3.867342
C	-1.067227	-2.904007	2.713773	H	-2.397841	0.775204	3.839935
C	-1.993543	-2.050090	3.548070	H	2.397841	-0.775204	3.839935
C	1.992464	-4.106264	0.000000	H	2.397684	-2.944920	2.592442
C	-1.370236	-3.600151	-1.574123	H	-2.398333	-3.718773	1.249933
C	-0.292551	-3.918657	-0.713824	H	-2.304205	-2.574584	4.459388
C	1.066365	-3.807050	-1.156123	H	-2.892405	-1.741876	3.012359
C	1.369374	-3.165286	-2.327337	H	2.892705	-3.490341	0.000000
C	0.291751	-2.576794	-3.031415	H	2.300686	-5.158474	0.000000
C	-1.067227	-2.904007	-2.713773	H	-2.398333	-3.718773	-1.249933
C	0.291915	-1.339286	-3.743448	H	2.397684	-2.944920	-2.592442
C	1.369692	-0.435172	-3.898534	H	2.397841	-0.775204	-3.839935
C	1.066940	0.899975	-3.867342	H	-2.397841	0.775204	-3.839935
C	-0.291915	1.339286	-3.743448	H	-2.304205	-2.574584	-4.459388
C	-1.369692	0.435172	-3.898534	H	-2.892405	-1.741876	-3.012359
C	-1.066940	-0.899975	-3.867342	H	2.892405	1.741876	-3.012359
C	-1.993543	-2.050090	-3.548070	H	2.304205	2.574584	-4.459388
C	1.993543	2.050090	-3.548070	H	-2.397684	2.944920	-2.592442
C	-1.369374	3.165286	-2.327337	H	2.398333	3.718773	-1.249933
C	-0.291751	2.576794	-3.031415	H	2.398333	3.718773	1.249933
C	1.067227	2.904007	-2.713773	H	-2.397684	2.944920	2.592442
C	1.370236	3.600151	-1.574123	H	-2.300686	5.158474	0.000000
C	0.292551	3.918657	-0.713824	H	-2.892705	3.490341	0.000000
C	-1.066365	3.807050	-1.156123	H	2.892405	1.741876	3.012359
C	0.292551	3.918657	0.713824	H	2.304205	2.574584	4.459388

Table S16. Cartesian coordinates of optimized structure of [6]CPP^{2+} in S_1.

C	-2.30320	-3.34660	1.24120	C	3.44180	-2.35390	-0.01810
C	-1.04400	-3.90680	1.24010	C	2.90440	-2.86400	-1.24120
C	-0.33740	-4.11070	0.01870	C	1.77200	-3.64790	-1.23990
C	-1.12580	-4.08630	-1.17240	C	1.11270	-3.97520	-0.01820
C	-2.38150	-3.52230	-1.17350	C	1.88300	-3.80520	1.17360
C	-2.92820	-2.95160	0.01870	C	3.01070	-3.01690	1.17510
C	-3.77760	-1.77910	-0.01590	H	-2.75150	-3.09130	2.19420
C	-3.98140	-1.06510	-1.23990	H	-0.55180	-4.06620	2.19230
C	-4.11510	0.30230	-1.24030	H	-0.70930	-4.43040	-2.11270
C	-4.05200	1.04330	-0.01600	H	-2.91360	-3.43890	-2.11470
C	-4.28160	0.28570	1.18000	H	-3.90160	-1.57720	-2.19190
C	-4.14920	-1.08050	1.17980	H	-4.13680	0.81980	-2.19240
C	-3.44180	2.35390	0.01810	H	-4.47770	0.79180	2.11890
C	-3.01070	3.01690	-1.17510	H	-4.24480	-1.61520	2.11850
C	-1.88300	3.80520	-1.17360	H	-3.51820	2.83590	-2.11620
C	-1.11270	3.97520	0.01820	H	-1.53800	4.22190	-2.11340
C	-1.77200	3.64790	1.23990	H	-1.31980	3.90000	2.19200
C	-2.90440	2.86400	1.24120	H	-3.30090	2.53360	2.19410
C	0.33740	4.11070	-0.01870	H	0.55180	4.06620	-2.19230
C	1.04400	3.90680	-1.24010	H	2.75150	3.09130	-2.19420
C	2.30320	3.34660	-1.24120	H	2.91360	3.43890	2.11470
C	2.92820	2.95160	-0.01880	H	0.70940	4.43040	2.11270
C	2.38150	3.52230	1.17350	H	4.24480	1.61520	-2.11850
C	1.12580	4.08630	1.17240	H	4.47770	-0.79190	-2.11890
C	3.77760	1.77910	0.01590	H	4.13680	-0.81980	2.19240
C	4.14920	1.08050	-1.17980	H	3.90160	1.57730	2.19190
C	4.28160	-0.28570	-1.18000	H	3.30090	-2.53370	-2.19410
C	4.05200	-1.04330	0.01600	H	1.31980	-3.90000	-2.19200
C	4.11510	-0.30230	1.24030	H	1.53800	-4.22190	2.11340
C	3.98140	1.06520	1.23990	H	3.51820	-2.83590	2.11620

Excited State 1: Singlet-A 1.7324 eV 715.69 nm f=**0.2078** <S**2>=0.000
118 ->121 -0.29878
119 ->120 0.64993

Table S17. Cartesian coordinates of optimized structure of [6]MCPP^{2+} in S_1.

C	-3.07780	2.60580	0.29930	C	-1.57980	-3.60300	1.37210
C	-2.75710	2.93080	-1.06830	C	-3.79520	1.36270	0.29930
C	-1.60240	3.61680	-1.37570	C	-3.91610	0.92250	-1.06820
C	-0.73220	3.92940	-0.30060	C	-3.61640	2.08810	-1.99380
C	-1.17580	3.82790	1.06430	C	-3.94920	0.44480	1.37390
C	-2.36000	3.19850	1.37390	C	-3.90230	-0.89550	1.06430
C	0.71360	3.92900	-0.29970	C	-3.76850	-1.33040	-0.30070
C	1.14940	3.81630	1.06250	C	-3.93260	-0.42040	-1.37580
C	-0.01060	4.13220	1.98920	C	-3.58320	-2.05670	1.98910
C	1.57980	3.60300	-1.37210	H	-1.28820	3.74660	-2.40710
C	2.73000	2.90360	-1.06240	H	-2.63660	3.00340	2.40580
C	3.04550	2.58250	0.29980	H	-0.01340	3.53340	2.90400
C	2.33000	3.16970	1.37220	H	-0.00440	5.19010	2.28850
C	3.58320	2.05670	-1.98910	H	1.26890	3.73440	-2.40430
C	3.90230	0.89550	-1.06430	H	2.59930	2.96610	2.40440
C	3.76850	1.33040	0.30070	H	3.06580	1.75490	-2.90370
C	3.94920	-0.44480	-1.37390	H	4.49630	2.59080	-2.28880
C	3.79520	-1.36270	-0.29930	H	3.91840	-0.78180	-2.40580
C	3.91610	-0.92250	1.06820	H	3.88780	0.75740	2.40710
C	3.93260	0.42040	1.37580	H	3.10660	-1.79390	2.91500
C	3.07780	-2.60580	-0.29930	H	4.53590	-2.61880	2.27910
C	2.75710	-2.93080	1.06830	H	2.63660	-3.00340	-2.40580
C	3.61640	-2.08810	1.99380	H	1.28820	-3.74660	2.40710
C	2.36000	-3.19850	-1.37390	H	0.01340	-3.53340	-2.90400
C	1.17580	-3.82790	-1.06430	H	0.00440	-5.19010	-2.28850
C	0.73220	-3.92940	0.30060	H	-2.59930	-2.96610	-2.40440
C	1.60240	-3.61680	1.37570	H	-1.26890	-3.73440	2.40430
C	0.01060	-4.13220	-1.98920	H	-3.10660	1.79390	-2.91500
C	-1.14940	-3.81630	-1.06250	H	-4.53590	2.61880	-2.27910
C	-0.71360	-3.92900	0.29970	H	-3.91840	0.78180	2.40580
C	-2.33000	-3.16970	-1.37220	H	-3.88780	-0.75740	-2.40710
C	-3.04550	-2.58250	-0.29980	H	-4.49630	-2.59080	2.28880
C	-2.73000	-2.90360	1.06240	H	-3.06580	-1.75490	2.90370

Excited State 1: Singlet-AU 1.8063 eV 686.38 nm f=**0.2164** <S**2>=0.000
136 ->139 -0.26628
137 ->138 0.66274

6. NMR, ESR, and HRMS spectra

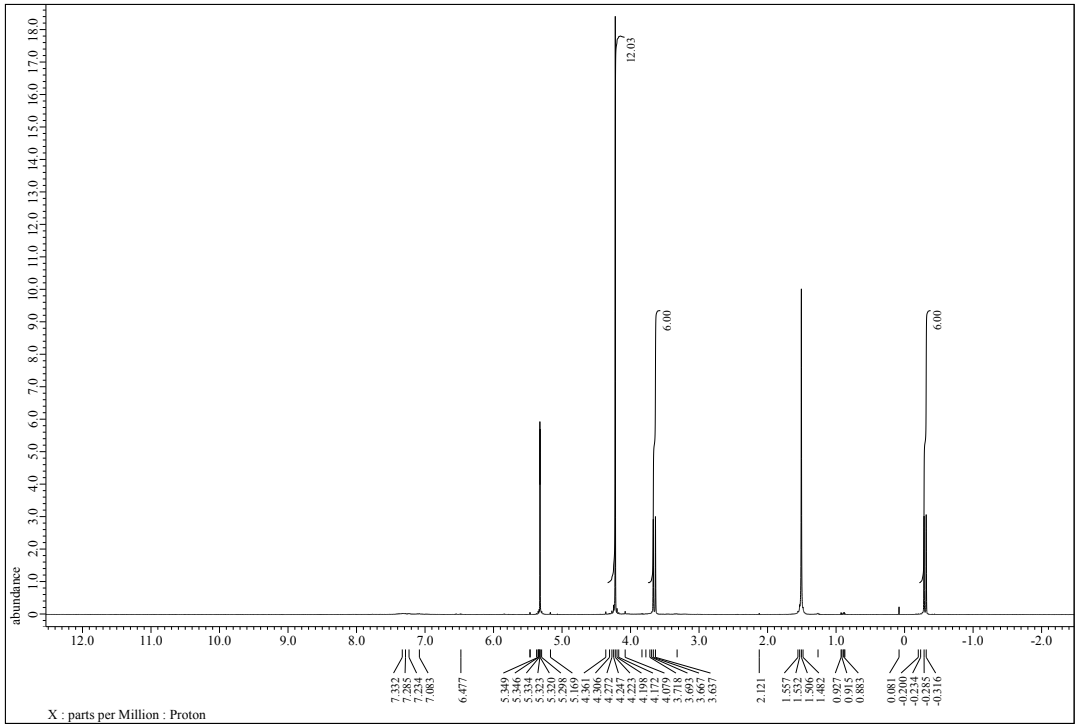

Figure S11. ^{1}H NMR spectrum of **2** (600 MHz, CD_2Cl_2). Reference: $CDHCl_2$ (5.32 ppm)

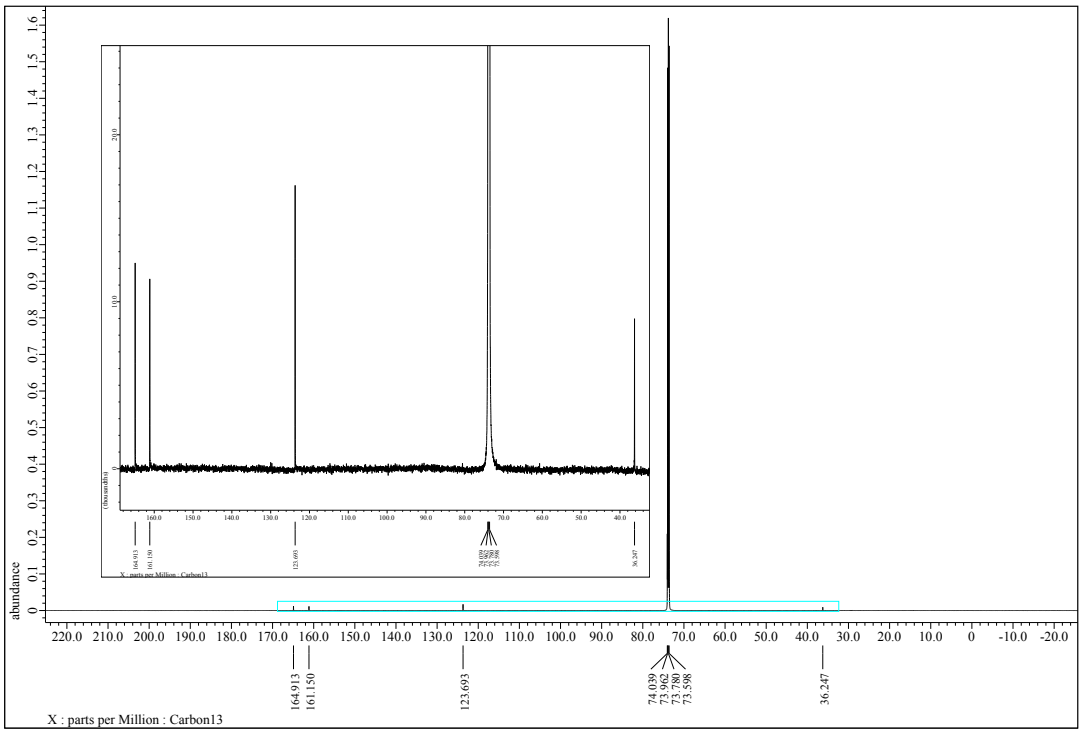

Figure S12. ^{13}C NMR spectrum of **2** (150 MHz, $C_2D_2Cl_4$). Reference: $C_2D_2Cl_4$ (73.78 ppm).

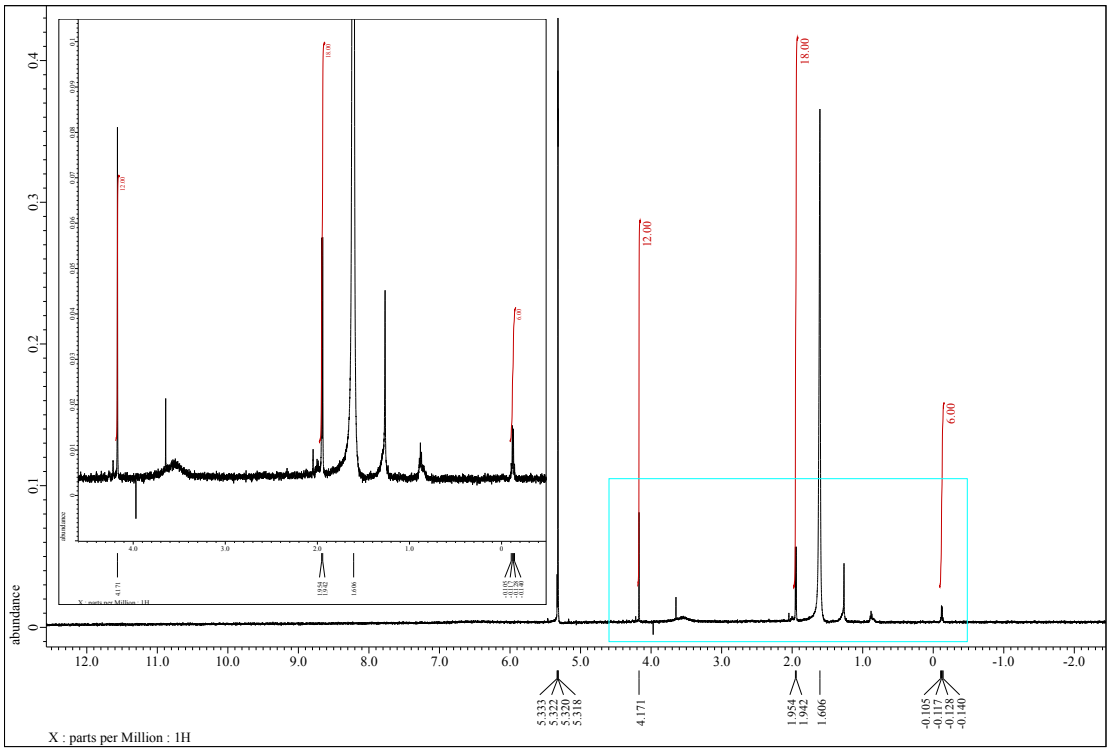

Figure S13. ^{1}H NMR spectrum of **3** (600 MHz, CD_2Cl_2). Reference: $CDHCl_2$ (5.32 ppm)

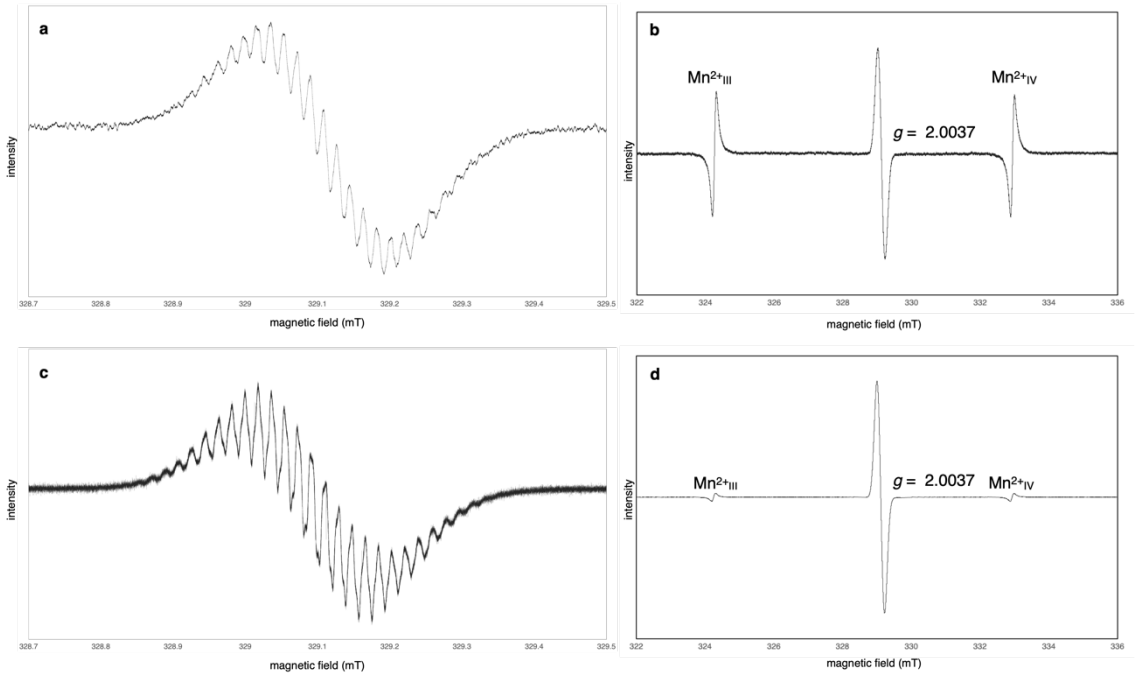

Figure S14. ESR spectra of [6]MCPP^{+}·SbCl$_6^-$ (**1**) in (a) and (b), and [6]MCPP^{+}·SbF$_6^-$ (**1′**) in (c) and (d). These samples were filtered using a syringe filter to prevent contamination by solids. Panels (a) and (b) were measured consecutively on the same [6]MCPP^{+}·SbCl$_6^-$ sample, while (c) and (d) were measured consecutively on the same [6]MCPP^{+}·SbF$_6^-$ sample. The spectrum (a) was integrated 30 times, whereas the spectra (b), (c), and (d) were not integrated. Additionally, (a) and (c) were not calibrated using standard substances. In contrast, the *g*-values (b) and (d) were determined using an external Mn^{2+} standard.

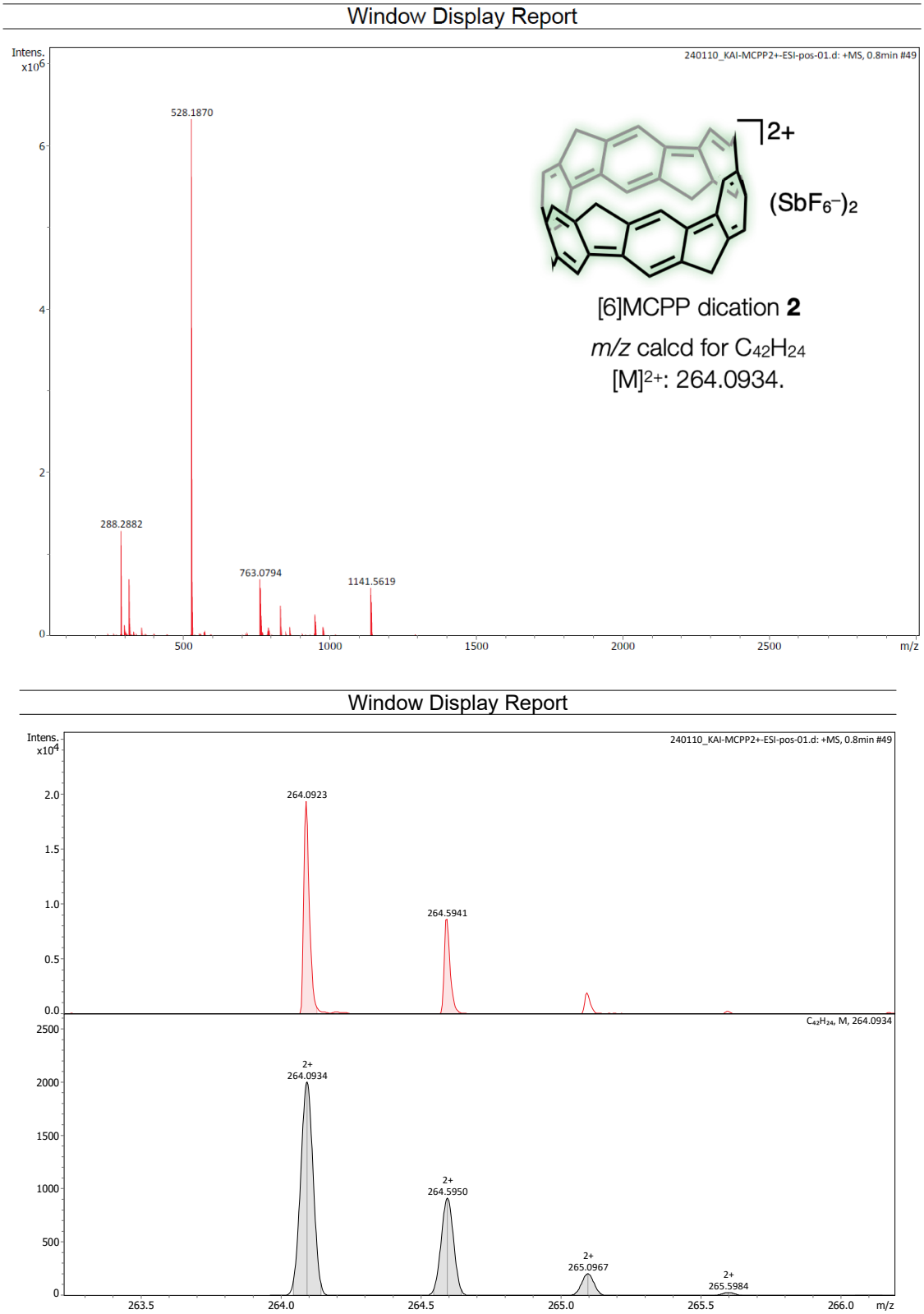

Figure S15. ESI mass spectrum of **2** (positive). Dissolving solvent: chloroform, no additives, type of detectors: Q/TOF, mass/charge ratios: +1, +2.

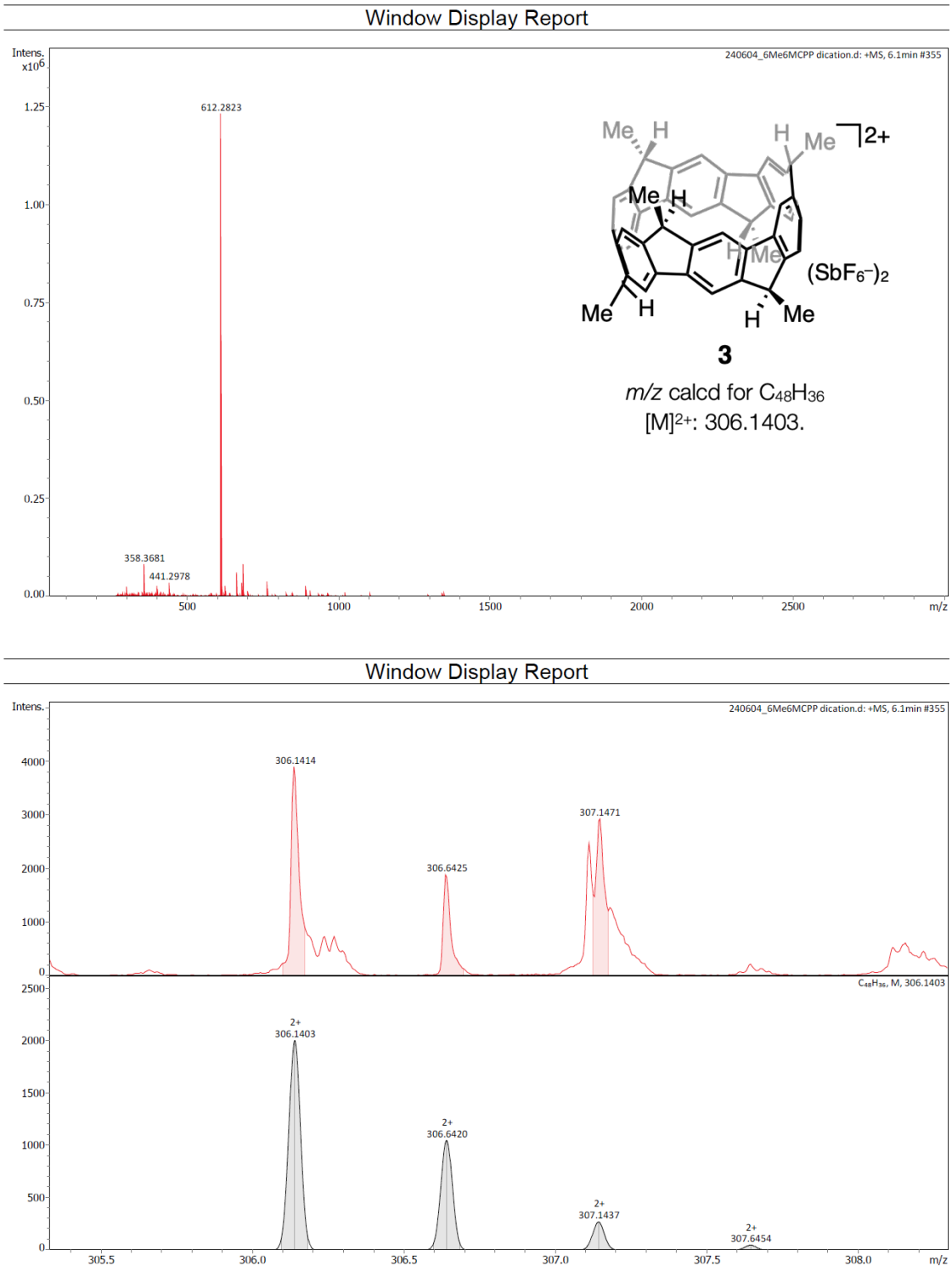

Figure S16. ESI mass spectrum of **3** (positive). Dissolving solvent: chloroform and methanol, no additives, type of detectors: Q/TOF, mass/charge ratios: +1, +2.

Supplementary References

S1 G. M. Sheldrick, *Acta Crystallogr. Sect. Found. Adv.* 2015, **A71**, 3–8.

S2 G. M. Sheldrick, *Acta Crystallogr. Sect. C Struct. Chem.* 2015, **C71**, 3–8.

S3 O. V. Dolomanov, L. J. Bourhis, R. J. Gildea, J. A. K. Howard and H. Puschmann, *J. Appl. Crystallogr.* 2009, **42**, 339–341.

S4 M. J. Frisch, G. W. Trucks, H. B. Schlegel, G. E. Scuseria, M. A. Robb, J. R. Cheeseman, G. Scalmani, V. Barone, G. A. Petersson, H. Nakatsuji, X. Li, M. Caricato, A. V. Marenich, J. Bloino, B. G. Janesko, R. Gomperts, B. Mennucci, H. P. Hratchian, J. V. Ortiz, A. F. Izmaylov, J. L. Sonnenberg, D. Williams-Young, F. Ding, F. Lipparini, F. Egidi, J. Goings, B. Peng, A. Petrone, T. Henderson, D. Ranasinghe, V. G. Zakrzewski, J. Gao, N. Rega, G. Zheng, W. Liang, M. Hada, M. Ehara, K. Toyota, R. Fukuda, J. Hasegawa, M. Ishida, T. Nakajima, Y. Honda, O. Kitao, H. Nakai, T. Vreven, K. Throssell, J. A. Montgomery, Jr., J. E. Peralta, F. Ogliaro, M. J. Bearpark, J. J. Heyd, E. N. Brothers, K. N. Kudin, V. N. Staroverov, T. A. Keith, R. Kobayashi, J. Normand, K. Raghavachari, A. P. Rendell, J. C. Burant, S. S. Iyengar, J. Tomasi, M. Cossi, J. M. Millam, M. Klene, C. Adamo, R. Cammi, J. W. Ochterski, R. L. Martin, K. Morokuma, O. Farkas, J. B. Foresman, D. J. Fox, Gaussian 16, Revision C.01, Gaussian, Inc., Wallingford CT, **2019**.

S5 D. Becke, *J. Chem. Phys.* 1993, **98**, 5648–5652.

S6 C. Lee, W. Yang and R. G. Parr, *Phys. Rev. B,* 1988, **37**, 785–789.

S7 X. Du, D. Zhang, Y. Guo, J. Li, Y. Han and C. Chen, *Angew. Chem. Int. Ed.* 2021, **60**, 13021–13028.

S8 Y. Li, Y. Segawa, A. Yagi and K. Itami, *J. Am. Chem. Soc.* 2020, **142**, 12850–12856.

S9 a) E. Kayahara, T. Kouyama, T. Kato and S. Yamago, *J. Am. Chem. Soc.* 2016, **138**, 338–344. b)Y. Masumoto, N. Toriumi, A. Muranaka, E. Kayahara, S. Yamago and M. Uchiyama, *J. Phys. Chem. A,* 2018, **122**, 5162–5167.